Classical Theory of the Scattering of Intense Laser Radiation by Free Electrons

E. S. SARACHIK AND G. T. SCHAPPERT
National Aeronautics and Space Administration, Electronics Research Center, Cambridge, Massachusetts 02139
(Received 14 January 1970)

A complete discussion of the classical theory of high-intensity Thomson scattering by free electrons is presented. Neglecting the radiation reaction, the equations of motion for an electron in an arbitrarily intense, elliptically polarized, plane electromagnetic wave can be solved exactly. From the solutions for the electron motion, the radiated power, momentum, and harmonics are calculated in two special Lorentz frames: the laboratory frame and the frame in which the electron is on the average at rest. The difference between the radiated power measured by an observer and that emitted by the electron is discussed for each frame. A sum rule for the radiated harmonics is derived. The limitation due to the neglect of radiation reaction is considered. Finally, the high- and low-intensity behavior of the spectrum and angular distribution of the radiation is analyzed in both frames.

I. INTRODUCTION

DURING the last ten years, the problem of the interaction of free electrons with intense electromagnetic fields has received considerable attention. The reason for this interest has been the development of high-power optical lasers capable of producing radiation fields whose power densities are many orders of magnitude greater than those possible with any other device. Thus the possibility naturally arises of the existence of effects that occur at large field intensities but at low photon energies. We refer the reader to a recent excellent review article by Eberly[1] for background and for a complete list of references. It should be borne in mind that not a single one of these effects can be said to have been unambiguously observed—indeed, most of these experiments have not yet been attempted.

In this paper, we present a complete discussion of the classical theory of high-intensity Thomson scattering from free electrons and the associated effects of harmonic production and intensity-dependent frequency shifts. While there have been several papers on this subject in the literature, none have presented detailed calculations as to what can be *observed* in the laboratory. The classical calculations[2] have been carried out (in perturbation theory) in the frame in which the electron is on the average at rest (the R frame). The quantum-mechanical calculations, expecially the one of Brown and Kibble,[3] while performed exactly, refer to the radiation emitted by the electron in the laboratory frame (the L frame). The radiation emitted by the electron in the L frame is not the same as the radiation seen by an observer in the L frame. The difference is due to the net motion of the average center of mass of the electron with respect to the observer. The distinction between the electron's point of view (retarded time) and the observer's is rather subtle and has not been sufficiently discussed in the literature in connection with this problem. We might mention that the classical and quantum-mechanical treatments of this problem have been shown to be equivalent for high intensities and are reviewed in an article by Kibble.[4]

As a preliminary to the problem, let us recall what is meant by high-intensity electromagnetic radiation. In the usual classical treatment of Thomson scattering,[5] the electron is assumed to be set in motion by the electric force $e\mathbf{E}$ and the radiation produced by the subsequent motion is calculated by the nonrelativistic Larmor radiation formula. At high intensities, however, the full force $e\mathbf{E}+(e/c)(\mathbf{v}\times\mathbf{B})$ must be used to calculate the electron motion. The motion then becomes a nonlinear function of the driving field in addition to becoming relativistic. The problem therefore becomes vastly more complicated. The parameter characterizing this high-intensity region will be called q^2, and is defined by

$$q^2=2e^2\langle\mathbf{A}^2(t)\rangle/m^2c^4=2Ir_0\lambda^2/\pi mc^3.$$

The first expression is in terms of the square of the vector potential and the second in terms of the intensity (measured in W/cm^2). The classical electron radius is r_0, the wavelength of the radiation is λ, c is the velocity of light, and e and m are the electron charge and mass, respectively. To get a feeling for the magnitude of q^2 and the intensities involved, we list these quantities for several typical electromagnetic-field-producing devices in Table I. The high-intensity effects are defined as those for which q^2 is at least of order unity. We see from Table I that the high-intensity region can be entered if diffraction-limited focussing can be approached. The field of high-intensity laser development is undergoing rapid expansion and there seems no reason why values of q^2 several orders of magnitude greater than those shown here could not become available.

The plan of the paper is as follows. In Sec. II we discuss the classical motion of an electron in an elliptically polarized electromagnetic wave. The wave is as-

[1] J. H. Eberly, *Progress in Optics*, edited by E. Wolf (North-Holland, Amsterdam, 1969), Vol. 7.
[2] Vachaspati, Phys. Rev. **128**, 664 (1962); **130**, 2598(E) (1963).
[3] L. S. Brown and T. W. B. Kibble, Phys. Rev. **133**, A705 (1964).
[4] T. W. B. Kibble, in *Cargèse Lectures in Physics*, edited by M. Lévy (Gordon and Breach, New York, 1968), p. 299.
[5] J. D. Jackson, *Classical Electrodynamics* (Wiley, New York, 1962).

sumed to be a pulse in the vector potential containing a large number of optical cycles. We then specialize the solution to two cases: motion in the R frame and motion in the L frame. Neglecting the radiation reaction, the electron motion can be solved exactly for arbitrary incident field intensity.

In Sec. III we discuss the radiation problem based on the solutions for the electron motion in the two frames of reference. In particular, we calculate the harmonic production as seen by observers in both frames and how they are related, and we show how the intensity-dependent frequency shift comes about. The relation between the power radiated by the electron and the power observed in each frame is stressed. The section closes with an estimate of the radiation reaction and the conditions under which it may be neglected in the equations of motion.

Section IV is devoted to a detailed analysis of the results of Sec. III. We present a discussion of the angular distribution of the power in each harmonic, the distribution of harmonics, and the total power observed in the L frame. These results are presented for both high and low intensities in the case of incident circular polarization, and for low intensities in the case of linear polarization. Some exact results, valid for arbitrary elliptically polarized incident radiation, are pointed out.

In the Sec. V we consider the limitations of our work due to quantum-mechanical and other effects.

II. ELECTRON EQUATIONS OF MOTION

We want to consider the motion of an electron, initially at rest at the origin, under the action of a laser beam incident upon it. The incident beam will be assumed to be transverse, plane, and arbitrarily elliptically polarized, and to be characterized by a wave vector $\mathbf{k}$ with frequency $\omega = c\,|\,\mathbf{k}\,| = ck$. In order that the initial conditions be realistically included, the plane wave will be multiplied by a pulse-shape factor, so that the vector potential is written

$$\mathbf{A}(\mathbf{r}, t) = \mathbf{A}(\eta)P(\eta), \tag{2.1}$$

where

$$\eta = \omega t - \mathbf{k}\cdot\mathbf{r} \tag{2.2}$$

is the Lorentz-invariant phase. We will assume that $\mathbf{A}(\eta)$ is periodic in η, and $P(\eta)$, the pulse-shape factor, is zero before and after the electron interaction with the laser beam. Thus, $P(\pm\infty)=0$ and $P_{\max}=1\approx P(0)$. For mathematical convenience, we will further assume that $P(\eta)$ is square integrable.

If we neglect the radiative reaction effects, the fully relativistic equation of motion for the electron in the plane-wave field may be solved exactly.[6–8] The Hamilton-Jacobi equation for this problem is

$$[\nabla S(\mathbf{r}, t) - (e/c)\mathbf{A}(\eta)P(\eta)]^2 - (1/c^2)[\partial S(\mathbf{r}, t)/\partial t]^2 + m^2c^2 = 0, \tag{2.3}$$

where $S(\mathbf{r}, t)$ is the Hamilton principal function. We look for a solution in the standard form

$$S(\mathbf{r}, t) = \boldsymbol{\alpha}\cdot\mathbf{r} + \beta ct + \Phi(\eta), \tag{2.4}$$

where $\boldsymbol{\alpha}$ and β are constants determined by the boundary conditions and $\Phi(\eta)$ is a function determined by (2.3). This function is easily found to be

$$\Phi(\eta) = \tfrac{1}{2}(\boldsymbol{\alpha}\cdot\mathbf{k} + \beta k)^{-1}\int_{\eta_0}^{\eta}[\alpha^2 - \beta^2 + m^2c^2 - 2(e/c)\boldsymbol{\alpha}\cdot\mathbf{A}(\eta)P(\eta) + (e^2/c^2)A^2(\eta)P^2(\eta)]d\eta. \tag{2.5}$$

The equation for the motion is obtained by differentiating the principal function with respect to the constants $\boldsymbol{\alpha}$ and equating this to the initial coordinate:

$$\nabla_\alpha S = \mathbf{r}_0 = \mathbf{r}(\eta) + \int_{\eta_0}^{\eta}\frac{\boldsymbol{\alpha} - (e/c)\mathbf{A}(\eta)P(\eta)}{\boldsymbol{\alpha}\cdot\mathbf{k} + \beta k}d\eta - 2\mathbf{k}\int_{\eta_0}^{\eta}\frac{\alpha^2 - \beta^2 + m^2c^2 - 2(e/c)\boldsymbol{\alpha}\cdot\mathbf{A}(\eta)P(\eta) + (e^2/c^2)A^2(\eta)P^2(\eta)}{(2\boldsymbol{\alpha}\cdot\mathbf{k} + 2\beta k)^2}d\eta, \tag{2.6}$$

and, with $\mathbf{r} - \mathbf{r}_0$ given by this equation,

$$ct_0 = \partial S/\partial\beta = ct - (\mathbf{k}/k)\cdot(\mathbf{r} - \mathbf{r}_0) - k^{-1}(\eta - \eta_0), \tag{2.7}$$

which just reflects the definition (2.2).

The canonical momenta and energy are given by differentiating the principal function with respect to the coordinates:

$$\begin{aligned}\mathbf{P}_{\mathrm{can}} &= \mathbf{p} + (e/c)\mathbf{A} = \nabla S\\ &= \boldsymbol{\alpha} - \mathbf{k}\left[\frac{\alpha^2 - \beta^2 + m^2c^2 - 2(e/c)\boldsymbol{\alpha}\cdot\mathbf{A}(\eta)P(\eta) + (e^2/c^2)A^2(\eta)P^2(\eta)}{2(\boldsymbol{\alpha}\cdot\mathbf{k} + \beta k)}\right],\end{aligned} \tag{2.8}$$

[6] L. D. Landau and E. M. Lifshitz, *Classical Theory of Fields*, 2nd ed. (Addison-Wesley, Reading, Mass., 1962).
[7] J. J. Sanderson, Phys. Letters **18**, 114 (1965).
[8] J. H. Eberly and A. Sleeper, Phys. Rev. **176**, 1570 (1968).

TABLE I. Characteristics of some typical electromagnetic-field-producing devices.

Device	Wavelength (cm)	Power or energy	Pulse length	Diffraction-focused intensity (W/cm²)	q^2
Microwave tube	3	10^4 J	10^{-2} sec	10^5	7×10^{-5}
He-Ne laser	6.3×10^{-5}	50 mJ/sec	CW	10^7	3×10^{-12}
High-brightness Nd Q-switched glass laser system	10^{-4}	60 J	30 nsec	10^{17}	0.14
High-brightness Nd mode-locked glass laser system	10^{-4}	80 J	3 psec	4×10^{21}	3000

and, in terms of this result,

$$E=-\partial S/\partial t=-c[\beta+(\mathbf{k}/k)\cdot(\boldsymbol{\alpha}-\mathbf{P}_{\text{can}})]. \quad (2.9)$$

The complete solutions are obtained by imposing boundary conditions on the electron. There are two common boundary conditions treated in the literature: the lab frame (quantities denoted by subscript L) in which the electron is initially at rest, and the "on the average at rest" or center-of-momentum frame (subscript R), in which the electron undergoes periodic motion about a fixed center. We discuss these frames in turn.

A. Lab Frame

The electron is sitting at the origin before the laser beam is turned on. Thus, at $t=-\infty$, $\mathbf{P}_{\text{can}}=0$, $\mathbf{r}=0$, and $E=mc^2$. Evaluating (2.8) at $\eta=-\infty$ therefore yields

$$\boldsymbol{\alpha}_L=\tfrac{1}{2}\mathbf{k}_L[(\alpha_L^2-\beta_L^2+m^2c^2)/(\boldsymbol{\alpha}_L\cdot\mathbf{k}_L+\beta_Lk_L)], \quad (2.10)$$

which is consistent with $\mathbf{r}_0=0$ in (2.6). Noting that $\boldsymbol{\alpha}_L\times\mathbf{k}_L=0$, we see that $\boldsymbol{\alpha}_L$ has no transverse part and the longitudinal part is given by

$$[\boldsymbol{\alpha}_L\cdot(\mathbf{k}_L/k_L)+\beta_L]^2=m^2c^2. \quad (2.11)$$

The initial energy condition applied to (2.9) then fixes the sign so that

$$\boldsymbol{\alpha}_L\cdot(\mathbf{k}_L/k_L)+\beta_L=-mc. \quad (2.12)$$

Thus (2.12) and the fact that $\boldsymbol{\alpha}$ is longitudinal are the only constraints on these constants. This arbitrariness can be traced to the arbitrary way in which the principal function can be separated into the form (2.4). Since $\boldsymbol{\alpha}_L$ and β_L always enter in the combination given in (2.12), we can, without loss of generality, choose $\boldsymbol{\alpha}_L=0$ and $\beta_L=-mc$ to simplify the algebra.

The equation of motion (2.6) now becomes

$$k_L\mathbf{r}(\eta)=-\int_{-\infty}^{\eta}\left[\frac{e\mathbf{A}(\eta')P(\eta')}{mc^2}-\frac{1}{2}\frac{\mathbf{k}_L}{k_L}\frac{e^2A^2(\eta')P^2(\eta')}{m^2c^4}\right]d\eta'. \quad (2.13)$$

The form of $\mathbf{r}(\eta)$ looks deceptively simple—the lab-frame time t is in fact hidden in (2.13) through the defining equation $\eta=\omega_Lt-\mathbf{k}_L\cdot\mathbf{r}$, so that the orbit $\mathbf{r}(t)$ may be quite complicated. In particular, although the motion will contain no higher than second harmonic oscillations in terms of η, $\mathbf{r}(t)$ may contain *all* multiples of ω_L.

The momentum and energy are obtained by using the $\boldsymbol{\alpha}_L$ and β_L in (2.8) and (2.9), yielding

$$\mathbf{p}(\eta)=-\frac{e}{c}\mathbf{A}(\eta)P(\eta)+\frac{\mathbf{k}_L}{2k_L}\frac{e^2A^2(\eta)P^2(\eta)}{mc^3} \quad (2.14)$$

and

$$E(\eta)=mc^2[1+e^2A^2(\eta)P^2(\eta)/2m^2c^4]. \quad (2.15)$$

Equations (2.13)–(2.15) now provide a complete solution to the electron motion problem in the lab frame. As the electromagnetic wave overlaps the electron, the electron acquires a harmonic motion transverse to the beam direction due to the first term in (2.14), and an acceleration along the beam direction due to the growth of $P^2(\eta)$ multiplying the zero-frequency part of $A^2(\eta)$. There will also be a longitudinal harmonic due to the 2η part of $A^2(\eta)$ which, as we shall see, vanishes in the particular case of circular polarization. After the $P(\eta)$ factor reaches its constant value in the center of the pulse, the electron is undergoing various harmonic motions about a center that itself is drifting with respect to the lab. As $P(\eta)$ turns off, the harmonic motion dies down and the center decelerates until at $\eta=+\infty$, corresponding to $t=+\infty$, the pulse has passed and the electron is again at rest in the laboratory. It is now displaced from its original position by a distance $\mathbf{r}(\infty)$ in the beam direction. This net displacement is pulse shape dependent but is easily calculated. For example, using a normalized Gaussian pulse of width $T \gg \omega_L^{-1}$, the net displacement is

$$\mathbf{r}(\infty) = (\mathbf{k}_L/4k_L)[e^2\langle A^2(\eta)\rangle/m^2c^4](\tfrac{1}{2}\pi)^{1/2}Tc \approx q^2Tc, \tag{2.16}$$

where terms of order $\exp(-1/T^2\omega_L^2)$ have been neglected, and where q^2 is the previously defined intensity parameter.

To discuss the average motion along the beam direction, we *define* a drift velocity $(\mathbf{v}_D)$ as the velocity of the frame in which the average momentum is zero. The time average is to be taken over a (laboratory) time that is long compared to the optical period ω_L^{-1} but short compared to the pulse length T (since even picosecond pulses contain about 1000 optical cycles, this is easy to do at optical frequencies). Since $\mathbf{p}$ and E in (2.14) and (2.15) form a four-vector and η is invariant under Lorentz transformation, $\mathbf{v}_D$ is the velocity of the Lorentz transformation that transforms the average three-momentum to zero:

$$\langle\mathbf{P}(\eta)\rangle - (v_D/c^2)\langle E(\eta)\rangle = 0, \tag{2.17}$$

which is solved to become

$$\mathbf{v}_D = (\mathbf{k}_L/k_L)\{q^2P^2(\eta)c/[4+q^2P^2(\eta)]\}. \tag{2.18}$$

We can follow the buildup and decline of $\mathbf{v}_D$ with the onset and retreat of the pulse explicitly from (2.18) in accordance with our previous discussion. It is easy to see that an electron at rest entering the leading edge of the laser pulse and picking up the velocity $\mathbf{v}_D$ takes a time $(1-v_D/c)^{-1}T$ to have the trailing edge of the pulse catch up to it and therefore it travels a distance $\frac{1}{4}q^2Tc$ in the lab. This motion of the center of momentum was first noted by Brown and Kibble[3] and most recently by Eberly and Sleeper.[8] Finally we note from (2.15) that the increased velocity of the center of momentum causes the electron to gain mass.[9] When the electron is at the peak of the pulse, $\langle E^2\rangle - \langle p^2\rangle c^2 \equiv m^{*2}c^4$, so the new mass is $(m^*)^2 = m^2 + \Delta m^2$, where $\Delta m^2 = \frac{1}{2}q^2m^2$.

B. Average Rest Frame

We can most easily discuss the oscillatory motion of the electron by working in the frame in which the average momentum is zero (the R frame). This can be done by imposing different boundary conditions on (2.6) and (2.9) and solving for a new set of $\boldsymbol{\alpha}$'s and β's. To be specific, we consider a long pulse that has been turned on in the past and afterward remains constant at $P(\eta)=1$. During the pulse buildup, the velocity of the R frame with respect to the lab increases until it reaches v_D.

[9] T. W. B. Kibble, Phys. Rev. **138**, B740 (1965).

Applying the R-frame boundary conditions that $\langle\mathbf{p}_R\rangle = 0$ in (2.8) yields

$$\boldsymbol{\alpha}_R = \tfrac{1}{2}\mathbf{k}_R\left[\frac{\alpha_R^2 - \beta_R^2 + m^2c^2 + (e^2/c^2)\langle A^2(\eta)\rangle}{\boldsymbol{\alpha}_R\cdot\mathbf{k}_R + \beta_R k_R}\right], \tag{2.19}$$

so that $\boldsymbol{\alpha}_R$ again is longitudinal, with only the combination

$$\left(\frac{\mathbf{k}_R}{k_R}\cdot\boldsymbol{\alpha}_R + \beta_R\right) = -\left(m^2c^2 + \frac{e^2}{c^2}\langle A^2(\eta)\rangle\right)^{1/2} = -m^*c \tag{2.20}$$

being determined. The electron motion in the R frame becomes

$$k_R\mathbf{r}_R(\eta) = -\frac{e}{m^*c}\int^\eta \mathbf{A}(\eta')d\eta' + \frac{\mathbf{k}_R}{2k_R}\frac{e^2}{m^{*2}c^4}\int^\eta [A^2(\eta') - \langle A^2(\eta)\rangle]d\eta'. \tag{2.21}$$

The integrals have been left indefinite since the initial value is of no consequence for the present discussion.

The motion is seen to be purely oscillatory with the transverse motion taking place at the frequency of $\mathbf{A}(\eta)$ and the longitudinal motion at twice this frequency. The zero-frequency part of $A^2(\eta)$ has been subtracted out in (2.21) and $\mathbf{r}_R(\eta)$ is purely oscillatory.

The position, time, and frequency in the R frame are, of course, related to the corresponding quantities in the lab frame by a Lorentz transformation. For example, the frequency of the laser beam in the R frame is given by the Doppler shift of the lab frame frequency (at the peak of the pulse):

$$\omega_L^2 = \omega_R^2[1 + e^2\langle A^2(\eta)\rangle/m^2c^4]. \tag{2.22}$$

C. Invariants

We will need some quantities that are the same in the L and R frames—these are Lorentz invariants of the problem. We first consider the electron proper time and then the electron four-velocity and acceleration.

The phase η is invariant. We will show that the proper time interval $d\tau$ of the electron, also an invariant, is proportional to an interval $d\eta$. In any arbitrary frame, we have, from the definition (2.2),

$$d\eta = [\omega(dt/d\tau) - \mathbf{k}\cdot(d\mathbf{r}/d\tau)]d\tau$$
$$= (1/mc)[\omega(E/c) - c\mathbf{k}\cdot\mathbf{p}]d\tau.$$

Now substituting the general expressions (2.8) and (2.9) for the energy and momentum gives

$$mcd\eta = -[\beta + (\mathbf{k}/k)\cdot\boldsymbol{\alpha}]\omega d\tau, \tag{2.23}$$

and we see that the form of the proportionality factor depends on the frame we are in, although the numerical value is the same for all frames.

For the specific case of the L and R frame, we find

$$d\eta = \omega_L d\tau = \omega_R(1 + \tfrac{1}{2}q^2)^{1/2}d\tau, \tag{2.24}$$

which simply reflects the Doppler shift (2.22).

We can now easily calculate the various four-vectors by differentiating the coordinates with respect to τ, or, equivalently, η. For example, the square of the four-acceleration, an invariant that proves useful in the discussion of the radiation, can be invariantly expressed as

$$a_\mu a^\mu = (d^2r_\mu/d\tau^2)(d^2r^\mu/d\tau^2) = c^2\omega^2\left(\frac{\mathbf{k}\cdot\boldsymbol{\alpha}+k\beta}{kmc}\right)^2\left(\frac{e}{mc^2}\frac{d\mathbf{A}(\eta)}{d\eta}\right)^2, \quad (2.25)$$

where (2.6), (2.7), and (2.24) have been used. This expression can be evaluated in terms of the quantities of any frame by using the appropriate $\boldsymbol{\alpha}$ and β.

D. Examples

Consider an elliptically polarized plane wave traveling along the $+z$ direction:

$$\mathbf{A}(\eta) = A_0[\hat{e}_x\,\delta\cos\eta + \hat{e}_y(1-\delta^2)^{1/2}\sin\eta], \quad (2.26)$$

where $\hat{e}_x$ and $\hat{e}_y$ are the transverse unit vectors and the constant parameter δ characterizes the degree of elliptic polarization. Linear polarization corresponds to $\delta=0$, ±1 and circular polarization to $\delta=\pm2^{-1/2}$. In terms of the A_0 defined by (2.26), the intensity parameter becomes $q^2=e^2A_0^2/m^2c^4$.

In the lab frame, we may insert (2.26) directly into (2.6) with $P(\eta)=1$ and obtain

$$k_L\mathbf{r}_L = \hat{e}_x(-q\delta\sin\eta) + \hat{e}_y[q(1-\delta^2)^{1/2}\cos\eta] + \tfrac{1}{4}q^2\hat{e}_z[\eta+\tfrac{1}{2}(2\delta^2-1)\sin2\eta]. \quad (2.27)$$

Then, using the definition of η, the z motion is written

$$k_Lz_L = v_Dk_Lt + (v_D/2c)(2\delta^2-1)\sin2\eta, \quad (2.28)$$

and we see explicitly that the electron drifts with velocity v_D and has second harmonic oscillations (in η) in the z direction. Note that in the case of circular polarization, the oscillating z motion vanishes so that the resulting orbit is helical.

We can perform the same operations in the R frame and find[2]

$$k_R\mathbf{r}_R = -2a[\hat{e}_x\,\delta\sin\eta - \hat{e}_y(1-\delta^2)^{1/2}\cos\eta] + \hat{e}_z\tfrac{1}{2}a^2(2\delta^2-1)\sin2\eta, \quad (2.29)$$

where the motion in R frame is characterized by the parameter

$$a^2 = q^2(4+2q^2)^{-1}. \quad (2.30)$$

For linearly polarized laser light, $\delta=1$, the orbit in the R frame can be found by eliminating η from (2.29):

$$16k_R^2z^2 = k_R^2x^2(4a^2-k_R^2x^2). \quad (2.31)$$

The orbit is a "figure eight" in the xz plane and is shown in Fig. 1 for various field intensities $0\le a^2\le0.5$. The velocity as a function of orbit position is

$$v_R^2 = c^2[1-4(1-2a^2)(2+2a^2-k_R^2x^2)^{-2}], \quad (2.32)$$

so that the electron moves fastest on the straight part of the orbit and slowest on the round part. As a^2 gets small, the orbit shrinks into a one-dimensional harmonic oscillator common in low-intensity treatments of Thomson scattering.

For circular polarization in the R frame, the orbit is a circle of radius $\sqrt{2}ak_R^{-1}$ in the xy plane and the electron orbits with constant velocity $\sqrt{2}\,ac$.

Finally, we conclude this section by noting that we can no longer apply the superposition principle to the electron motion. We cannot describe the linear polarization case, say, as a linear combination of the right and left circularly polarized cases, since there would be no way of generating any oscillatory z motion by

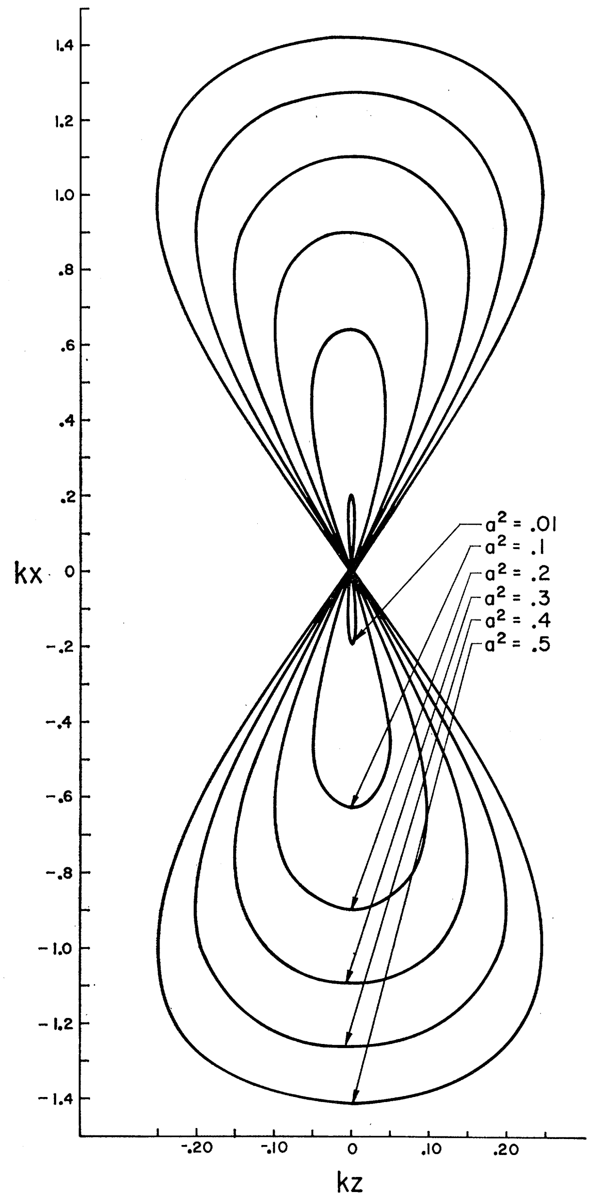

FIG. 1. Orbital motion of the electron in the R frame for incident linearly polarized light for various values of the intensity.

circularly polarized light alone. The failure of superposition is not surprising because of the nonlinearity of the problem—we have essentially solved for the electron motion under the complete nonlinear

$$e[\mathbf{E}+(\mathbf{v}/c)\times\mathbf{B}]$$

force.

III. RADIATION

We now turn to the radiation problem associated with the electron motion discussed in the Sec. II. As is well known, there are two different, but equivalent, ways of looking at the radiation problem. First, one can compute the electromagnetic fields radiated by the source and hence find the energy and momentum flow at a space-time point (x, t) a large distance from the source. Second, one can calculate the energy-momentum loss rate of the source directly in terms of its velocity and acceleration without any reference to the radiated fields. If the source remains on the average at rest with respect to an observer, the rate of energy loss of the source equals the power measured by the observer. On the other hand, if there is a net average motion between the observer and the source, the relationship between the emitted power and the observed power is more subtle. Both situations will arise in the next few sections.

In Secs. III A and III B we discuss the production and angular distribution of harmonics in the R and L frame, respectively. Obviously, this requires the radiation-field point of view. In Sec. III C we calculate the energy-momentum loss rate of the charge directly and compare with the results of Secs. III A and III B. Section III D discusses the radiation reaction.

A. Harmonic Production in R Frame

The general formula for the radiation fields generated by an arbitrary electron motion are easily written down. However, since we are primarily interested in the scattered power, it is convenient to work directly with the radiation intensity. Furthermore, since the electron motion is harmonic in the R frame, we take as our starting point the expression for the average power per unit solid angle radiated into the mth harmonic (final polarization not measured)[5]:

$$dP_R^{(m)}/d\Omega_R=[e^2\omega_R^4m^2/(2\pi c)^3]\times\left|\int_0^{2\pi/\omega_R}\mathbf{n}\times\left(\mathbf{n}\times\frac{d\mathbf{r}_R}{dt}\right)\exp\left[im\omega_R\left(t-\frac{\mathbf{n}}{c}\cdot\mathbf{r}_R(t)\right)\right]dt\right|^2. \quad (3.1)$$

The vector $\mathbf{n}$ is a unit vector in the direction of observation and $\mathbf{r}_R(t)$ is the electron coordinate in the average rest frame. The Fourier transform in (3.1) is with respect to the observer's time in the R frame; however, the integral is expressed in terms of the retarded time of the source. This accounts for the $(\mathbf{n}/c)\cdot\mathbf{r}_R$ in the exponential. ω_R is the frequency of the incident field.

Since our equations of motion are expressed in terms of the parameter η, it is convenient to change the time variable to η, i.e.,

$$\omega_Rt=\eta+\mathbf{k}_R\cdot\mathbf{r}_R(\eta). \quad (3.2)$$

We then define a vector $\mathbf{J}$ representing the integral

$$\mathbf{J}=\int_0^{2\pi}k_R\frac{d\mathbf{r}_R(\eta)}{d\eta}\times\exp\{i[\eta+\mathbf{k}_R\cdot\mathbf{r}_R(\eta)-k_R\mathbf{n}\cdot\mathbf{r}_R(\eta)]\}d\eta, \quad (3.3)$$

so that

$$dP_R^{(m)}/d\Omega_R=(e^2\omega_R^2m^2/8\pi^3c)[|\mathbf{J}|^2-|\mathbf{n}\cdot\mathbf{J}|^2]. \quad (3.4)$$

If the general solution for $k_R\mathbf{r}(\eta)$, (2.29), in terms of its x-y-z components is substituted into the above integral, the components of the integral $\mathbf{J}$ become

$$J_x=-2a\delta\pi\chi_1^m, \quad (3.5a)$$

$$J_y=-2a(1-\delta^2)^{1/2}\pi\chi_2^m, \quad (3.5b)$$

$$J_z=a^2(2\delta^2-1)\pi\chi_3^m, \quad (3.5c)$$

where

$$\chi_{(1,2,3)}^m=\pi^{-1}\int_0^{2\pi}(\cos\eta,\sin\eta,\cos2\eta)\times\exp[im\varphi(\eta)]d\eta, \quad (3.6)$$

with

$$\varphi(\eta)=\eta+a^2(2\delta^2-1)\sin^2\tfrac{1}{2}\theta\sin2\eta+2a[\delta\sin\eta\cos\alpha-(1-\delta^2)^{1/2}\cos\eta\cos\beta] \quad (3.7)$$

and (see Fig. 2)

$$\cos\alpha=\mathbf{n}\cdot\hat{e}_x=\sin\theta\cos\varphi, \quad (3.8a)$$

$$\cos\beta=\mathbf{n}\cdot\hat{e}_y=\sin\theta\sin\varphi, \quad (3.8b)$$

$$\cos\theta=\mathbf{n}\cdot\hat{e}_z. \quad (3.8c)$$

In general, χ_j^m is a rather complicated function of a, θ, φ, and δ, and is not expressible in simple form. Making repeated use of the generating function for a Bessel function[10]

$$\exp(i\rho\cos\psi)=\sum_{n=-\infty}^{n=+\infty}(i)^n\exp(in\psi)J_n(\rho), \quad (3.9)$$

one can express the integrand in (3.6) as a triple sum over Bessel functions. The integral over η then collapses the triple sum to a double sum, with the result

$$\begin{pmatrix}\chi_1^{(m)}\\ \chi_2^{(m)}\\ \chi_3^{(m)}\end{pmatrix}=-\sum_{n,l=-\infty}^{\infty}J_l[ma^2(2\delta^2-1)\sin^2(\tfrac{1}{2}\theta)]\times(-i)^nJ_{n-2l-m}(z_1)\begin{pmatrix}iJ_{n+1}(z_2)-iJ_{n-1}(z_2)\\ J_{n+1}(z_2)+J_{n-1}(z_2)\\ J_{n+2}(z_2)+J_{n-2}(z_2)\end{pmatrix}, \quad (3.10)$$

[10] G. N. Watson, *A Treatise on the Theory of Bessel Functions*, 2nd ed. (Cambridge U.P., Cambridge, England, 1965).

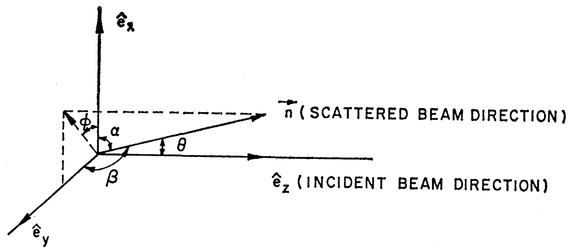

FIG. 2. Angular geometry. θ is the scattering angle of the scattered light.

where $z_1=2am(1-\delta^2)^{1/2}\cos\beta$ and $z_2=2am\delta\cos\alpha$. One now applies the Graf addition theorem[11] to the sum over n,

$$\sum_{n=-\infty}^{\infty}(-i)^n J_n(z_2)J_{n+p}(z_1)=[(z_1+iz_2)/(z_1-iz_2)]^{p/2}J_p((z_1^2+z_2^2)^{1/2}),\quad(3.11)$$

and this reduces $\chi^{(m)}$ to a single sum over l. The final result is

$$\begin{pmatrix}\chi_1^{(m)}\\ \chi_2^{(m)}\\ \chi_3^{(m)}\end{pmatrix}=\sum_{l=-\infty}^{\infty}J_l[ma^2(2\delta^2-1)\sin^2(\tfrac{1}{2}\theta)]\times\begin{pmatrix}f^{m+1+2l}J_{m+2l+1}(\rho)+f^{m+2l-1}J_{m+2l-1}(\rho)\\ -if^{m+2l+1}J_{m+2l+1}(\rho)+if^{m+2l-1}J_{m+2l-1}(\rho)\\ f^{m+2l+2}J_{m+2l+2}(\rho)+f^{m+2l-2}J_{m+2l-2}(\rho)\end{pmatrix},\quad(3.12)$$

where

$$f=-i(z_1-iz_2)/(z_1+iz_2)=-(i/\rho^2)(2am\sin\theta)^2[(1-\delta^2)^{1/2}\sin\varphi-i\delta\cos\varphi]^2\quad(3.13)$$

and

$$\rho^2=z_1^2+z_2^2=(2am\sin\theta)^2(\delta^2\cos^2 2\varphi+\sin^2\varphi).\quad(3.14)$$

Substituting the expressions for J into (3.4) gives the power per unit solid angle radiated into the nth harmonic in terms of the previously given χ's:

$$\begin{aligned}dP_R^{(n)}/d\Omega_R=[A(\omega_R^2)n^2/(1+\tfrac{1}{2}q^2)]&\times[\delta^2|\chi_1^n|^2+(1-\delta^2)|\chi_2^n|^2\\&+\tfrac{1}{4}a^2(2\delta^2-1)^2|\chi_3^n|^2\\&-|\delta\cos\varphi\sin\theta\,\chi_1^n\\&+(1-\delta^2)^{1/2}\sin\varphi\sin\theta\,\chi_2^n\\&-\tfrac{1}{2}a\cos\theta\,(2\delta^2-1)\chi_3^n|^2],\end{aligned}\quad(3.15)$$

where $A(\omega_R^2)=e^2\omega_R^2q^2/8\pi c$. We note that in the limit $q^2\to 0$, (3.15) reduces to

$$dP_R^{(n)}/d\Omega_R=A(\omega_R^2)\delta_{n,1}[\delta^2\sin^2\alpha+(1-\delta^2)\sin^2\beta],\quad(3.16)$$

which is the usual classical Thomson scattering result. Our general result (3.15) therefore constitutes the intensity corrections to ordinary Thomson scattering in the R frame and is exact to all orders of q^2, the intensity parameter of the incident laser beam.

Because the expressions (3.12) contain infinite sums, the general result for nth harmonic scattering cannot usually be expressed in a tractable form. Only for the case of a circularly polarized incident laser beam does the sum in (3.12) collapse and in this case to a single Bessel function. Thus, for incident circular polarization, the result becomes[12]

$$\begin{aligned}dP_R^{(n)}/d\Omega_R=2n^2A(\omega_R^2)/(1+\tfrac{1}{2}q^2)&\times[(\cot^2\theta/2a^2)J_n^2(2^{1/2}an\sin\theta)\\&+J_n'^2(2^{1/2}an\sin\theta)],\end{aligned}\quad(3.17)$$

which corresponds to synchrotron radiation from an electron in circular motion with radius $\sqrt{2}\,ak_R^{-1}$ and velocity $\sqrt{2}\,ac$.

It is important to realize that even though the electron motion is periodic in the proper time with frequency ω_R ($\delta^2=\frac{1}{2}$) or ω_R and $2\omega_R$ ($\delta^2=1$, 0), the radiation contains *all* the harmonics. This is due to both the retarded time factor $\mathbf{n}\cdot\mathbf{r}$ in the exponent of (3.1) and the relation between the retarded time and the proper time.

The closed form expression (3.17) for incident circular polarization can be summed over n and integrated over solid angles to give the total power radiated in the R frame:

$$P_R=\int d\Omega_R\sum_{n=1}^{\infty}\frac{dP_R^{(n)}}{d\Omega_R}=B(\omega_R^2)(1+\tfrac{1}{2}q^2),\quad(3.18)$$

where $B(\omega^2)=e^2\omega^2q^2/3c$. This result provides us with a convenient sum rule for the harmonics. While for arbitrary incident polarization this summation and integration cannot be carried out explicitly, we will derive an expression for the total power radiated in the R frame. Equation (3.18) will then be a special case of this more general result.

B. Harmonic Production in L Frame

In the Sec. III A we calculated the angular distribution of the harmonics radiated in the average rest frame R. In the L frame, the motion of the electron is *not* periodic and hence one does not have pure harmonic generation. We could again calculate the radiation from the fields generated by the motion in the L frame, but since the motion in the L and R frames differ only by a drift velocity in the incident beam direction, we can more simply Lorentz-transform the R-frame results into the L frame.

[11] W. Magnus, F. Oberhettinger, and R. P. Soni, *Formulas and Theorems for the Special Functions of Mathematical Physics* (Springer-Verlag, New York, 1966).

[12] J. Hanus and J. Ernest, Phys. Letters **16**, 262 (1965).

Consider the expression for the total average power observed in a solid-angle element $d\Omega_R$ in the R frame:

$$dP_R = \sum_{n=1}^{\infty} (dP_R^{(n)}/d\Omega_R)\, d\Omega_R. \qquad (3.19)$$

Associated with this energy per unit time is a momentum per unit time given by $c^{-1}dP_R$. But we know that energy and momentum per unit *proper* time are the components of a four-vector. Therefore, to transform (3.19) into the L frame, we first Lorentz-transform the energy-momentum per proper time interval and then correct for the time intervals.

The L frame moves uniformly with a drift velocity v_D in the negative z direction with respect to the R frame. Hence the Lorentz transformation requires that

$$dP_L = \gamma_D dP_R (1+\beta_D \cos\theta_R)\, dt_R/dt_L. \qquad (3.20)$$

We now evaluate the right-hand side of (3.20) in terms of the L-frame quantities. With

$$\beta_D = v_D c^{-1} = q^2(4+q^2)^{-1}, \qquad (3.21)$$

one finds

$$\gamma_D = (1-\beta_D^2)^{-1/2} = (1+\tfrac{1}{4}q^2)(1+\tfrac{1}{2}q^2)^{-1/2}. \qquad (3.22)$$

The frequency seen at the angle θ_L in the L frame satisfies

$$\omega_L^2 = \omega_R^2 (1+\tfrac{1}{2}q^2)[1+\tfrac{1}{2}q^2 \sin^2(\tfrac{1}{2}\theta_L)]^{-2}, \qquad (3.23)$$

whereas the relation between the incident frequencies ($\theta=0$) is

$$\omega_L^0 = \omega_R^0 (1+\tfrac{1}{2}q^2)^{1/2}. \qquad (3.24)$$

We must now distinguish the frequency of the incident radiation from the scattered frequency in each frame. We will only use the notation ω^0 for the incident frequency when confusion is likely to arise.

Angles in the two frames are related by

$$\cos\theta_R = (\cos\theta_L - \beta_D)(1-\beta_D \cos\theta_L)^{-1}, \qquad (3.25)$$

so that the solid-angle ratio becomes

$$d\Omega_R/d\Omega_L = (1+\tfrac{1}{2}q^2)[1+\tfrac{1}{2}q^2 \sin^2(\tfrac{1}{2}\theta_L)]^{-2}. \qquad (3.26)$$

The evaluation of dt_R/dt_L is more subtle. The Δt refers to the observer's time interval, which is related to the electron's retarded time interval $\Delta t'$ through

$$\Delta t = \Delta t' - (1/c)\mathbf{n}\cdot\Delta\mathbf{r}(t'), \qquad (3.27)$$

with all times measured in the same frame. $\mathbf{r}(t')$ is known from the equations of the electron motion in a given frame and $\mathbf{n}$ is a unit vector in the direction of the observer from the origin of the $\mathbf{r}$ coordinate system. Since we are dealing with optical frequencies, we can only measure energies over a time interval containing many optical cycles—we must therefore average. In the R frame $\langle \mathbf{r}_R(t')\rangle = 0$, so that

$$\Delta t_R = \Delta t_R', \qquad (3.28)$$

while in the L frame there is a contribution to $\langle \mathbf{r}_L\rangle$ from the uniform drift motion to give

$$\Delta t_L = \Delta t_L'(1-\beta_D \cos\theta_L). \qquad (3.29)$$

On the other hand, the time intervals associated with the electron motion (retarded times) in different frames are related by the Lorentz time dilation

$$\Delta t_L' = \gamma_D \Delta t_R', \qquad (3.30)$$

so that the effective time interval ratio for two *observers* in the two frames becomes

$$dt_L/dt_R = \gamma_D(1-\beta_D \cos\theta_L). \qquad (3.31)$$

This distinction between the transformation for an observer's time interval and the corresponding electron's retarded time interval was recently pointed out by Ginzburg[13] in connection with interpreting synchrotron radiation in astrophysical problems.

The final expression for the average power per unit solid angle *observed* in the L frame becomes

$$\frac{dP_L}{d\Omega_L} = \frac{(1+\tfrac{1}{2}q^2)^2}{[1+\tfrac{1}{2}q^2 \sin^2(\tfrac{1}{2}\theta_L)]^4} \sum_{n=1}^{\infty} \frac{dP_R^{(n)}}{d\Omega_R}, \qquad (3.32\text{a})$$

where all quantities inside $dP_R^{(n)}/d\Omega_R$ are to be expressed in terms of their L-frame values.

Similarly, if we calculate the average power per unit solid angle radiated by the electron in terms of its own retarded time in the L frame we do not correct for retardation but use dt_L' instead of dt_L in (3.20). This yields

$$\frac{dP_L'}{d\Omega_L} = \frac{(1+\tfrac{1}{2}q^2)^2(1+\tfrac{1}{4}q^2)^{-1}}{[1+\tfrac{1}{2}q^2 \sin^2(\tfrac{1}{2}\theta_L)]^3} \sum_{n=1}^{\infty} \frac{dP_R^{(n)}}{d\Omega_R}. \qquad (3.32\text{b})$$

The frequency spectrum of the scattered radiation in the L frame does not consist of simple multiples of the frequency of the incident radiation. From (3.23), (3.24), and the R-frame result $\omega_R = n\omega_R^0$ we obtain

$$\omega_L^{(n)} = n\omega_L^0 [1+\tfrac{1}{2}q^2 \sin^2(\tfrac{1}{2}\theta_L)]^{-1}, \qquad (3.33)$$

which for $n=1$ is commonly called the intensity-dependent frequency shift. The meaning of nth harmonic in connection with the L-frame quantity $dP_L^{(n)}/d\Omega_L$ then must be understood in the sense of (3.33). For $q^2 \sim 1$ any frequency $\omega > \omega_L^0$ is radiated—we only have to look at the appropriate angle. At large q^2, however, the angular distribution in the L frame is sharply forward peaked so that only a small range of θ_L contributes to the angular distribution. We will discuss this in more detail in Sec. IV.

The relation (3.32a) between the average power observed in the L and R frames may be interpreted in a very physical way. Consider the number of photons observed with frequency ω_L in a solid angle $d\Omega_L$ and a time interval Δt_L. Clearly this same number of photons

[13] V. L. Ginzburg, V. N. Sazonov, and S. I. Syrovatskii, Usp. Fiz. Nauk 94, 63 (1968) [Soviet Phys. Usp. 11, 34 (1968)].

is observed in the R frame with frequency ω_R in the solid angle $d\Omega_R$ and time interval Δt_R. Hence

$$N=(\Delta t_L/\hbar\omega_L)(dP_L/d\Omega_L)d\Omega_L$$
$$=(\Delta t_R/\hbar\omega_R)(dP_R/d\Omega_R)d\Omega_R, \qquad (3.34)$$

which is equivalent to (3.32a). The relation between the power radiated and the power and number cross sections is given in the Appendix.

For the case of incident circular polarization, the solid angle integral over (3.32a) can be performed by transforming the integral back into R-frame variables. The result for the total power observed in the laboratory is

$$P_L=P_R\{(1+\tfrac{1}{4}q^2)^2(1+\tfrac{1}{2}q^2)^{-1}+\tfrac{1}{64}(1+\tfrac{1}{2}q^2)^{-3}[(23/4)q^4+\tfrac{5}{4}q^6+8q^2+3-(3\sqrt{2}/q)(1+\tfrac{1}{2}q^2)^{3/2}\times(1+2q^2)\ln((\sqrt{\tfrac{1}{2}})q+(1+\tfrac{1}{2}q^2)^{1/2})]\}, \qquad (3.35a)$$

and this reduces in the low- and high-q^2 limits to

$$P_L=P_R[1+(7/80)q^4], \qquad q^2\ll1 \qquad (3.35b)$$

and

$$P_L=P_R\tfrac{1}{8}q^2, \qquad q^2\gg1 \qquad (3.35c)$$

where $P_R=B(\omega_L^2)=(1+\frac{1}{2}q^2)B(\omega_R^2)$ is given in (3.18). The reasons for the difference between P_L and P_R will be discussed in more detail in Sec. IV.

C. Power Radiated by Electron

Up to now we have discussed the radiation problem from the electromagnetic field point of view and have calculated the power received by observers in different frames of reference. Let us now consider the source point of view and calculate the energy-momentum loss of the electron directly from its acceleration and velocity.

We begin the discussion with the energy-momentum four-vector rate at which radiation is leaving the charge[14]:

$$d\Pi^\mu/d\tau=\tfrac{2}{3}(e^2/c^4)a_\lambda a^\lambda(v^\mu/c). \qquad (3.36)$$

The $\mu=0$ component refers to the energy and the $\mu=1, 2, 3$ components to the momentum vector. a^μ and v^μ are the acceleration and velocity four-vectors of the electron:

$$v^\mu=dx^\mu/d\tau=(\gamma c, \gamma\mathbf{v}(\tau)), \qquad (3.37)$$

with

$$v_\mu v^\mu=-\gamma^2(c^2-\mathbf{v}^2)=-c^2 \qquad (3.38)$$

and

$$a^\mu=dv^\mu/d\tau. \qquad (3.39)$$

We have already calculated the invariant $a^\mu a_\mu$ from the equations of motion. With the vector potential (2.26) substituted into (2.25), we find

$$a_\mu a^\mu=\tfrac{1}{2}c^2(\omega_L^2)q^2[1-(2\delta^2-1)\cos2\eta]. \qquad (3.40)$$

This then gives, for the instantaneous energy-momentum loss *per proper time interval* of the electron evaluated in an arbitrary frame of reference specified by v^μ,

$$d\Pi^\mu/d\tau=B(\omega_L^2)[1-(2\delta^2-1)\cos2\eta](v^\mu/c^2). \qquad (3.41)$$

The time component is related to the invariant instantaneous energy emission rate

$$R=v_\mu(d\Pi^\mu/d\tau)=(c/\gamma)(d\Pi^0/d\tau)=c(d\Pi^0/dt'). \qquad (3.42)$$

This energy loss rate is with respect to the charge's retarded time—we must still distinguish the observer's time t from the electron's retarded time t'.

To obtain the average energy-momentum loss rate of the electron, we must average the instantaneous rates over times that are long compared to the periods of the motion. Thus the total energy-momentum lost by the charge along a world line containing many periods of the motion is

$$\Pi^\mu(A)-\Pi^\mu(B)=\int_{\tau_B}^{\tau_A}\frac{d\Pi^\mu}{d\tau}d\tau. \qquad (3.43)$$

The average energy-momentum loss rate in a given frame is then the value of the above integral in that frame, divided by the electron's time interval corresponding to the proper interval along the world line:

$$\left\langle\frac{\Delta\Pi^\mu}{\Delta t'}\right\rangle=[t'(\tau_A)-t'(\tau_B)]^{-1}\int_{\tau_B}^{\tau_A}\frac{d\Pi^\mu}{d\tau}d\tau. \qquad (3.44)$$

We can now easily evaluate the average using (2.24) and (2.29):

$$dt_R'/d\tau=\gamma_R=v_R^0/c=(1+\tfrac{1}{2}q^2)^{1/2}[1+a^2(2\delta^2-1)^2\cos2\eta] \qquad (3.45)$$

and

$$d\mathbf{r}_R/cd\tau=\gamma_R\boldsymbol{\beta}_R=(1+\tfrac{1}{2}q^2)^{1/2}[-2a\mathbf{e}_x\,\delta\cos\eta+2a\mathbf{e}_y(1-\delta^2)^{1/2}\sin\eta+a^2\mathbf{e}_z(2\delta^2-1)^2\cos2\eta], \qquad (3.46)$$

so that the average energy per unit time lost by the electron becomes

$$c\Delta\Pi_R^0/\Delta t_R'=B(\omega_R^2)[1+\tfrac{1}{2}q^2-\tfrac{1}{8}q^2(2\delta^2-1)^2] \qquad (3.47)$$

and the momentum lost per unit time,

$$\Delta\boldsymbol{\Pi}_R/\Delta t_R'=-\mathbf{e}_zB(\omega_R^2)(q^2/8c)(2\delta^2-1)^2. \qquad (3.48)$$

In the R frame there is no net average motion between observer and source. This results in equal-time intervals for observer and source, as shown in (3.27) and (3.28). Therefore we can equate the average rate of energy loss (3.47) with the total average observed power in the R frame given by the sum and solid-angle integral over (3.15). Hence (3.47) furnishes us with an exact sum rule for the harmonics even when the sum and integral over (3.15) cannot be performed. For

[14] F. Rohrlich, *Classical Charged Particles* (Addison-Wesley, Reading, Mass., 1965).

circularly polarized incident laser radiation in the R frame, the identity between power loss of the electron (3.47) and the power observed (3.18) is explicitly demonstrated. We also note that the R-frame momentum loss rate (3.47) is zero for incident circular polarization ($\delta^2=\frac{1}{2}$) which implies a symmetric angular distribution of the radiated energy with respect to the $\theta=\frac{1}{2}\pi$ plane.

In the L frame one again easily calculates (3.44). From (2.24) and (2.27) we find

$$dt_L'/cd\tau=\gamma_L=v_L{}^0/c=1+\tfrac{1}{4}q^2[1+(2\delta^2-1)\cos 2\eta] \tag{3.49}$$

and

$$d\mathbf{r}_L/cd\tau=\gamma_L\boldsymbol{\beta}_L=-q\mathbf{e}_x\,\delta\cos\eta-q\mathbf{e}_y(1-\delta^2)^{1/2}\sin\eta+\mathbf{e}_z\tfrac{1}{4}q^2[1+(2\delta^2-1)\cos 2\eta]. \tag{3.50}$$

The average rate of energy and momentum loss in the laboratory frame then become, respectively,

$$c\frac{\Delta\Pi_L{}^0}{\Delta t_L'}=B(\omega_L{}^2)\left[1-\frac{\frac{1}{8}q^2(2\delta^2-1)^2}{1+\frac{1}{4}q^2}\right] \tag{3.51}$$

and

$$\frac{\Delta\boldsymbol{\Pi}_L}{\Delta t_L'}=\mathbf{e}_z\frac{B(\omega_L{}^2)}{c}\frac{\frac{1}{4}q^2}{1+\frac{1}{4}q^2}[1-\tfrac{1}{2}(2\delta^2-1)^2]. \tag{3.52}$$

In the L frame, the average energy loss rate (3.51) is not equal to the total average power measured by an observer. In (3.29) we found that the retarded time interval is not equal to the observer's time interval, but is related to it by $\Delta t_L=\Delta t_L'(1-\beta_D\cos\theta_L)$. This implies a relation between the emitted and observed power of the form

$$P_L=\int\left(\frac{d}{d\Omega_L}c\frac{\Delta\Pi_L{}^0}{\Delta t_L}\right)\frac{d\Omega_L}{1-\beta_D\cos\theta_L}>c\frac{\Delta\Pi_L{}^0}{\Delta t_L'}. \tag{3.53}$$

The energy loss into a given solid angle, when integrated, satisfies

$$\Delta\Pi^0/\Delta t'=\int[(d/d\Omega)(\Delta\Pi^0/\Delta t')]d\Omega, \tag{3.54}$$

and because there is a net forward momentum loss, (3.52), the angular distribution in (3.54) is forward peaked. This accounts for the inequality in (3.53). The fact that the observed power radiated is larger than the energy loss rate of the source is explicitly demonstrated for circular polarization, where both rates have been calculated exactly [compare (3.35) with (3.51) after setting $\delta^2=\frac{1}{2}$].

The above situation must not be thought to violate conservation of energy. Because of the net relative motion between electron and observer, the energy stored in the region between the observer and the electron continuously changes. When the electron comes toward us, the stored energy decreases and the observer measures the rate of energy emission from the source plus the decrease of the stored field energy.[13] Because of the forward peaking of the radiation, we always observe more than the electron emits.

D. Radiation Reaction

Our equations of motion for the electron in an electromagnetic field have up to now neglected radiation reaction effects. We will now estimate under what conditions this neglect is justified. Our discussion is based on the Lorentz-Dirac equation

$$ma^\mu=F^\mu+\Gamma^\mu, \tag{3.55}$$

where

$$F^\mu=(e/c)(\partial^\mu A^\nu-\partial^\nu A^\mu)v_\nu, \tag{3.56}$$

in terms of the vector potential and the four-velocity (3.37), and

$$\Gamma^\mu=\tfrac{2}{3}(e^2/c^3)[(da^\mu/d\tau)-(1/c^2)a_\lambda a^\lambda v^\mu]. \tag{3.57}$$

Our previous discussion of the equations of motion corresponds to (3.55) without the Γ^μ.

The Abraham radiation reaction four-vector Γ^μ consists of two terms. We recognize the $a_\lambda a^\lambda v^\mu$ part as the negative of (3.36), the energy-momentum four-vector rate at which radiation is leaving the charge. Strictly speaking, this by itself is the radiation reaction. The $da^\mu/d\tau$ term, referred to as the Schott term, gives rise to a nonlocality in time in the formal solution of (3.55). In the nonrelativistic limit of the theory, the $da^\mu/d\tau$ term reduces to the familiar $d\mathbf{a}/dt$ damping force which is derivable by considering the energy transfer from the incident field to the scattered radiation. We note that there have been many misconceptions about radiation and radiation reaction which have only recently been clarified.[14]

For our purposes, it suffices to calculate Γ^μ and require that its magnitude be small compared to that of the driving force F^μ. From (3.37)–(3.40) we easily calculate the four-vector (expressed as a column matrix)

$$\Gamma^\mu=\tfrac{2}{3}(e^2/c^2)\omega_L{}^2\times\begin{bmatrix}-\frac{1}{2}q^2[1+(2\delta^2-1)\cos 2\eta]-\frac{1}{8}q^4[1-(2\delta^2-1)^2\cos^2 2\eta]\\ q\delta\cos\eta\{1+\frac{1}{2}q^2[1-(2\delta^2-1)\cos 2\eta]\}\\ q(1-\delta^2)^{1/2}\sin\eta\{1+\frac{1}{2}q^2[1-(2\delta^2-1)\cos 2\eta]\}\\ -\frac{1}{8}q^4[1-(2\delta^2-1)^2\cos^2 2\eta]\end{bmatrix}. \tag{3.58}$$

Similarly, the force due to the incident field becomes

$$F^\mu=mc\omega_Lq\begin{bmatrix}-(1-2\delta^2)\frac{1}{2}q\sin 2\eta\\ \delta\sin\eta\\ -(1-\delta^2)^{1/2}\cos\eta\\ -\frac{1}{2}q(1-2\delta^2)\sin 2\eta\end{bmatrix}. \tag{3.59}$$

Clearly one cannot require that each component of Γ^μ be less than the corresponding components of F^μ. For incident circular polarization F^0 and F^3 are zero but not Γ^0 and Γ^3. If we demand that the magnitude of the nonzero components of F^μ be greater than any of the components of Γ^μ, we obtain

$$r_0/\lambda_{0L} \ll 1, \qquad q^2<1 \tag{3.60a}$$

and

$$r_0 q^2/\lambda_{0L} \ll 1, \qquad q^2>1 \tag{3.60b}$$

where r_0 is the classical electron radius and λ_{0L} is the laboratory wavelength of the incident field. The above restriction must then be satisfied if the radiation reaction is to have a small effect on the electron motion. It should be realized, however, that even if this effect is small, it may, over a sufficiently long time, induce a significant alteration to the electron's motion. Such radiation pressure corrections have been discussed by Sanderson[7] and Kibble.[15]

IV. LOW- AND HIGH-INTENSITY BEHAVIOR

We have seen in Sec. III that the power observed in the laboratory frame is not the same as the power lost by the electron in that frame, the difference being due to the retardation effect introduced by the net motion of the electron's R frame with respect to the laboratory. Since the observed power is the experimentally important quantity, we will consider its behavior as a function of intensity and make specific low- and high-q^2 predictions.

Let us first note some exact results for arbitrary polarization and arbitrary intensity for forward and backward scattering.

In the forward direction, scattering takes place only at the incident frequency, all harmonics higher than $n=1$ not contributing:

$$(dP_L^{(n)}/d\Omega_L)(\theta=0)=\delta_{n,1}A(\omega_L^2). \tag{4.1}$$

In the backward direction, scattering occurs only at the odd harmonics (where $n=2s+1$):

$$(dP_L^{(n)}/d\Omega_L)(\theta=\pi)=A(\omega_L^2)[(2s+1)^2/(1+\tfrac{1}{2}q^2)^4] \times[(J_s+J_{s+1})^2-4\delta^2 J_s J_{s+1}]. \tag{4.2}$$

The arguments of all the Bessel functions appearing in (4.2) are $(2\delta^2-1)(2s+1)a^2$. For circular polarization, the expression in brackets becomes $\delta_{s,0}$, so that none of the harmonics higher than $n=1$ have either forward or backward scattering.

A. Circular Polarization

Next we consider in detail the low- and high-q^2 behavior of the L-frame observed power for the specific case of a circularly polarized incident beam. This case is, as we have already noted, the only incident polarization for which the infinite sum over Bessel functions in (3.10) degenerates into a single Bessel function. Using (3.17) and (3.32a), and expressing all angles in terms of L-frame angles, yields the explicit result for incident circular polarization:

$$dP_L^{(n)}/d\Omega_L=A(\omega_L^2)\{2n^2/[1+\tfrac{1}{2}q^2\sin^2(\tfrac{1}{2}\theta)]^4\} \times\left[\frac{2[\cos\theta-\frac{1}{2}q^2\sin^2(\frac{1}{2}\theta)]^2}{q^2\sin^2\theta}J_n^2(n\Theta)+J_n'^2(n\Theta)\right], \tag{4.3a}$$

where

$$\Theta=q\sin\theta/\sqrt{2}[1+\tfrac{1}{2}q^2\sin^2(\tfrac{1}{2}\theta)]. \tag{4.3b}$$

If we expand the Bessel functions for low q^2, we find the leading term

$$\frac{dP_L^{(n)}}{d\Omega_L}=A(\omega_L^2)\left[\frac{4(q^2)^{n-1}(n^2)^n}{8^n[(n-1)!]^2}\right](\sin^2\theta)^{n-1}(1+\cos^2\theta). \tag{4.4}$$

We see that the power observed at low q^2 is symmetric with respect to the $\theta=90°$ plane and that, except for $n=1$, it vanishes in the forward and backward direction in accordance with the discussion following (4.2).

The integral over the solid angle in (4.4) can be performed using the beta functions[11] $B(x,y)=\Gamma(x)\Gamma(y)/\Gamma(x+y)$:

$$2\int_0^1(\sin^2\theta)^{n-1}(1+\cos^2\theta)\,d(\cos\theta)=B(\tfrac{1}{2},n)+B(\tfrac{3}{2},n). \tag{4.5}$$

The total observed low-q^2 nth harmonic power is therefore

$$P_L^{(n)}=B(\omega_L^2)\left[\frac{3(n)^{2n+1}(q^2)^{n-1}(n+1)}{2^{n-1}(2n+1)!}\right]. \tag{4.6}$$

We note that in the low-q^2 limit, the leading term in $P_L^{(n)}$ is identical to the leading term in the corresponding result for the R frame $P_R^{(n)}$, since the Lorentz transformation between frames is itself at least of order q^2.

We can expand the observed power beyond the leading term and in so doing test the prediction (3.35b) for the total observed L-frame power to order q^4. The results will also provide specific experimental predictions for the low-intensity region. Thus, to order q^4, we have radiation only at the first three harmonics:

$$dP_L^{(1)}/d\Omega_L=A(\omega_L^2)\tfrac{1}{2}[1+\cos^2\theta-\tfrac{1}{8}q^2(11-4\cos\theta+6\cos^2\theta-12\cos^3\theta-\cos^4\theta)+(1/768)q^4(997-864\cos\theta+27\cos^2\theta-1248\cos^3\theta+891\cos^4\theta+192\cos^5\theta+5\cos^6\theta)], \tag{4.7a}$$

$$dP_L^{(2)}/d\Omega_L=A(\omega_L^2)q^2[1-\cos^4\theta-\tfrac{1}{6}q^2(13-6\cos\theta-6\cos^2\theta-9\cos^4\theta+12\cos^5\theta+2\cos^6\theta)], \tag{4.7b}$$

$$dP_L^{(3)}/d\Omega_L=A(\omega_L^2)q^4[1-\cos^2\theta-\cos^4\theta+\cos^6\theta]. \tag{4.7c}$$

[15] T. W. B. Kibble, Phys. Letters 20, 627 (1966).

Integrating over the solid angle gives the total power observed at the first three harmonics to order q^4:

$$P_L^{(1)}=B(\omega_L^2)[1-(6/5)q^2+(81/70)q^4], \quad (4.8a)$$

$$P_L^{(2)}=B(\omega_L^2)[(6/5)q^2-(83/35)q^4], \quad (4.8b)$$

$$P_L^{(3)}=B(\omega_L^2)[(729/560)q^4]. \quad (4.8c)$$

Summing these three expressions gives the total power observed in the L frame to order q^4:

$$P_L=B(\omega_L^2)[1+(7/80)q^4], \quad (4.9)$$

which agrees with our previous result (3.35b). Note that if we calculate the total power lost by the electron in the L frame according to (3.32b), we find that to order q^4 it agrees with the sum rule (3.51).

Turning now to the high-q^2 behavior, we find that if we consider nonforward angles (i.e., angles for which $q\gg1$ implies $q^2\sin^2(\frac{1}{2}\theta)\gg1$), there is very little radiation at any harmonic. To make this explicit, let us consider the three regions in which we have approximate expressions for the Bessel functions, namely, for $n\ll q$, for $n\sim q$, and for $n\gg q$. Using then the approximations to the Bessel functions for small argument and fixed order, for fixed argument and large order, and for large argument and large order, respectively, we find

$$\frac{dP_L^{(n)}}{d\Omega_L}=A(\omega_L^2)\frac{4(n^2)^n(\sin^2\theta)^{n-1}}{(q^2)^{n+3}[2\sin^4(\frac{1}{2}\theta)]^{n+1}[(n-1)!]^2}, \quad 1\ll n\ll q \quad (4.10a)$$

$$\frac{dP_L^{(n)}}{d\Omega_L}=A(\omega_L^2)\frac{16n^3(\frac{1}{2}e^2\sin^2\theta)^{n-1}}{\pi(q^2)^{n+3}[\sin^4(\frac{1}{2}\theta)]^{n+1}}, \quad n\sim q\gg1 \quad (4.10b)$$

$$\frac{dP_L^{(n)}}{d\Omega_L}=A(\omega_L^2)\frac{16n}{\pi q^6\sin^4(\frac{1}{2}\theta)\sin^2\theta}\times\exp\left[-2n\left(\ln\frac{\sqrt{2}\,q\sin\frac{1}{2}\theta}{\sin\theta}-1\right)\right], \quad n\gg q\gg1. \quad (4.10c)$$

We conclude that there are no significant amounts of radiation at high q^2 for any nonforward angles.

If we look, however, at forward angles (i.e., those for which $\theta\sim1/q$), the situation changes. We will see that at high q^2, essentially *all* the radiation is emitted at the *same* near forward angle $\theta_0=(\sqrt{8})/q$. This situation may be traced to the inevitable forward peaking of radiation emitted from a rapidly moving particle due to Lorenz transformation rather than to any intrinsic structure in the angular distribution.

In order to analyze the region $q^2\gg1$, $\theta\sim1/q$, we use the uniform asymptotic expansion of the Bessel functions[16] for $n>1$:

$$J_n(n\Theta)=\left(\frac{4\zeta}{1-\Theta^2}\right)^{1/4}\left(\frac{\zeta}{3\pi^2}\right)^{1/2}K_{1/3}(\tfrac{2}{3}n\zeta^{3/2})+O(n^{-5/3}), \quad (4.11a)$$

$$J_n'(n\Theta)=-\frac{2}{\Theta}\left(\frac{1-\Theta^2}{4\zeta}\right)^{1/4}\frac{\zeta}{\pi}K_{2/3}(\tfrac{2}{3}n\zeta^{3/2})+O(n^{-4/3}), \quad (4.11b)$$

where

$$\tfrac{2}{3}\zeta^{3/2}=\ln\left(\frac{1+(1-\Theta^2)^{1/2}}{\Theta}\right)-(1-\Theta^2)^{1/2} \quad (4.11c)$$

and the K's are the modified Bessel functions of the second kind related to the Airy functions.

The observed power at the nth harmonic (for n large enough for the first term of the uniform asymptotic expansions of the Bessel functions to be valid) is

$$\frac{dP_L^{(n)}}{d\Omega_L}=A(\omega_L^2)\frac{2n^2}{[1+\frac{1}{2}q^2\sin^2(\frac{1}{2}\theta)]^4}\frac{1}{\pi^2}(\tfrac{2}{3}\zeta^{3/2})\times\left[\frac{2[\cos\theta-\frac{1}{2}q^2\sin^2(\frac{1}{2}\theta)]^2}{q^2\sin^2\theta(1-\Theta^2)^{1/2}}K_{1/3}^2(\tfrac{2}{3}n\zeta^{3/2})+\frac{(1-\Theta^2)^{1/2}}{\Theta^2}K_{2/3}^2(\tfrac{2}{3}n\zeta^{3/2})\right]. \quad (4.12)$$

When the argument of the K functions becomes large compared to unity, the K functions appearing in (4.12) become exponentially small according to[16]

$$K_{1/3,2/3}(z)\rightarrow(\pi/2z)^{1/2}e^{-z}. \quad (4.13)$$

We see therefore that the power radiated at the higher harmonics will be negligible if the condition $n\frac{2}{3}\zeta^{3/2}\gg1$ obtains. We can verify from (4.10c) that, as a function of $q\theta$, $\frac{2}{3}\zeta^{3/2}$ is of order unity except near $q\theta=\sqrt{8}$. At $q\theta=\sqrt{8}$, $\Theta=1-1/q^2$ and $\frac{2}{3}\zeta^{3/2}$ becomes

$$\tfrac{2}{3}\zeta^{3/2}\,|_{\theta=\theta_0}=[\tfrac{1}{3}(\tfrac{1}{2}q^2)^{-3/2}]^{-1}\equiv n_0^{-1}. \quad (4.14)$$

Let us consider how the condition $n\frac{2}{3}\zeta^{3/2}\gg1$ may be violated. Away from forward directions, $\frac{2}{3}\zeta^{3/2}$ is itself of order unity so that for $n\gg1$ the condition holds and there is negligible radiation [we already know this from our discussion of (4.10)]. Near $\theta=\theta_0=(\sqrt{8})/q$, however, there will be significant amounts of radiation for all harmonics for which $n<n_0$, since our condition is there violated, but insignificant radiation for $n>n_0$, since there it is not. The radiation is thus confined to the near neighborhood of θ_0 and occurs only for those n's below the critical harmonic n_0, dropping off exponentially above the critical harmonic.

If we look precisely at the angle $\theta_0=(\sqrt{8})/q$, the magnitude of the observed radiated power in the nth harmonic is

$$\frac{dP_L^{(n)}}{d\Omega_L}(\theta=\theta_0)=A(\omega_L^2)\frac{n^2}{8\pi^2}\frac{1}{n_0}\left[\frac{(1-\Theta^2)^{1/2}}{\Theta^2}K_{2/3}^2\left(\frac{n}{n_0}\right)\right], \quad (4.15)$$

[16] *Handbook of Mathematical Functions*, edited by M. Abramowitz and I. A. Stengun (Dover, New York, 1965).

where the first term of (4.12) is of order q^{-2} smaller and has been neglected. Using the relation[16]

$$K_{2/3}(n/n_0)=\tfrac{1}{2}\Gamma(\tfrac{2}{3})(2n_0/n)^{2/3} \qquad (1\ll n<n_0) \quad (4.16)$$

gives the magnitude of the observed power at θ_0:

$$(dP_L{}^{(n)}/d\Omega_L)(\theta=\theta_0)=A(\omega_L{}^2)[(0.411)^2n^{2/3}/8] \qquad (1\ll n<n_0). \quad (4.17)$$

Notice that this expression is only trivially dependent on q^2 through the incident beam term $A(\omega_L{}^2)$. The power cross section corresponding to (4.17) (see the Appendix) is, in fact, independent of q^2.

We can estimate the *total* power at θ_0 by summing over n up to the critical harmonic n_0 using the approximate formula (for large n_0)

$$\sum_{n=1}^{n_0} n^{2/3}=\tfrac{3}{5}(n_0)^{5/3}$$

to obtain

$$(dP_L/d\Omega_L)(\theta=\theta_0)=A(\omega_L{}^2)(0.014)(q^2)^{5/2}. \quad (4.18)$$

The rapid increase in the total observed power with q^2, indicated by this expression, is due to the rapid opening up of new harmonics rather than to any increase in power radiated in the individual harmonics. The power observed in each harmonic is constant [aside from the trivial q^2 dependence in $A(\omega_L{}^2)$] but the number of radiating harmonics increases as q^3, thus leading to the q^5 dependence of the observed amplitude in (4.18). We will see below that the estimate (4.18) is quite a good approximation to the exact result.

We can summarize the essential features of the angular distributions for the observed power at high q^2 as follows.

(a) The radiation is confined to the region of the near forward angle $\theta_0=(\sqrt{8})/q$, all radiating harmonics peaking at this same angle.

(b) Near this peak angle, all harmonics below the critical harmonic $n_0=3(\frac{1}{2}q^2)^{3/2}$ radiate strongly. Thus as the intensity of the incident laser beam increases, the spectrum of the scattered radiation shifts upward.

(c) At the angle θ_0, the magnitude of $dP_L/d\Omega$ increases as $A(\omega_L{}^2)q^5$.

Let us now turn to the total power observed at a given angle. We can in fact sum (4.3) over all the harmonics using[10]

$$\sum_{n=1}^{\infty} n^2J_n{}^2(n\Theta)=\Theta^2(4+\Theta^2)/16(1-\Theta^2)^{7/2}, \quad (4.19a)$$

$$\sum_{n=1}^{\infty} n^2J_n'^2(n\Theta)=(4+3\Theta^2)/16(1-\Theta^2)^{5/2}. \quad (4.19b)$$

(Note that the first of these expressions is incorrectly given in Watson.[10]) The angular distribution for the total power observed in the laboratory frame thus becomes

$$dP_L/d\Omega_L=A(\omega_L{}^2)\{(1-\Theta^2)^{-7/2}/8[1+\tfrac{1}{2}q^2\sin^2(\tfrac{1}{2}\theta)]^4\} \times\left[\frac{[\cos\theta-\frac{1}{2}q^2\sin^2(\frac{1}{2}\theta)]^2}{[1+\frac{1}{2}q^2\sin^2(\frac{1}{2}\theta)]^2}(4+\Theta^2)+(1-\Theta^2)(4+3\Theta^2)\right]. \quad (4.20)$$

This result is valid for arbitrary q^2 and, in Fig. 3, we plot it for various values of the intensity.

At large q^2, (4.20) can be written

$$\frac{dP_L}{d\Omega_L}=\frac{A(\omega_L{}^2)}{128}\left[\left(\frac{7}{12}\right)^2\frac{5\theta^4}{4}(\tfrac{1}{2}q^2)^{7/2}\left(1+\frac{(\theta-\theta_0)^2}{(\Delta\theta)^2}\right)^{-7/2} +7(\tfrac{1}{2}q^2)^{5/2}\left(1+\frac{(\theta-\theta_0)^2}{(\Delta\theta)^2}\right)^{-5/2}\right], \quad (4.21)$$

where $\Delta\theta=(\sqrt{8})/q^2$. We again see that the first term is smaller than the second by a factor of q^{-2}. At the peak $\theta=\theta_0$, the estimate (4.18) is seen to agree quite well with (4.21).

If we integrate over the solid angle of the dominant term in (4.21), we get an estimate of the total observed power

$$P_L=B(\omega_L{}^2)\frac{7}{8\times 2^{5/2}}q^2, \quad (4.22)$$

which agrees favorably with (3.35c).

Up to now we have assumed that the polarization of the scattered radiation is not measured. Each term in (4.3a) does, however, correspond to a unique linear polarization direction. If we take $\mathbf{n}$ to be the direction of the observer, the linear polarization vector corresponding to the second term of (4.3a) is perpendicular to both $\mathbf{n}$ and the scattering plane (i.e., it is in the plane transverse to the initial beam direction). The polarization vector corresponding to the first term of (4.3a) is perpendicular to $\mathbf{n}$ and lies in the scattering plane. Since as we have seen, at high q^2 the second term of (4.3a) and (4.20) dominates near θ_0, we conclude that essentially all of the observed scattered radiation is linearly polarized in the plane transverse to the initial beam direction.

We have analyzed the observed scattered radiation, for circularly polarized incident radiation, by analyzing the radiation formula (4.3a). All the results we have obtained may be simply understood by recalling that an accelerating particle in relativistic motion synchrotron-radiates along its instantaneous direction. The motion at high q^2 for the case of circularly polarized incident radiation is a helix of pitch angle $\theta_P=v_Tv_D{}^{-1}$, where v_T is the transverse velocity and v_D is the longitudinal drift velocity. Inserting the previously found values of these quantities yields $\theta_P=(\sqrt{8})q^{-1}$. It is clear therefore that only an observer directly along the pitch of the helix sees anything at all. This explains the characteristic peaking at the near forward angle $(\sqrt{8})q^{-1}$. Similar arguments for the width of this peak and for the polarization of the observed radiation can be given to reinforce the analysis of this section.

B. Linear Polarization

We will briefly discuss the radiation produced by a linearly polarized incident laser beam. The mathematics for this situation is relatively intractable so that we can write the exact solution but can analyze it only in the case of low q^2. We expect many of the features of the incident circular polarization case to still apply here at high q^2, since many of those results were characteristic of the drift velocity which is the same in this case. The exact result can of course be put on a computer if more detailed high-q^2 results are desired.

The observed average power distribution in the laboratory frame for linearly polarized incident radiation is

$$\frac{dP_L^{(n)}}{d\Omega_L}=A(\omega_L^2)\frac{n^2}{[1+\frac{1}{2}q^2\sin^2(\frac{1}{2}\theta)]^4}\times\Bigg[\left(1-\frac{(1+\frac{1}{2}q^2)\cos^2\alpha}{[1+\frac{1}{2}q^2\sin^2(\frac{1}{2}\theta)]^2}\right)(F_1^n)^2-\tfrac{1}{2}q\frac{\cos\alpha[\cos\theta-\frac{1}{2}q^2\sin^2(\frac{1}{2}\theta)]}{[1+\frac{1}{2}q^2\sin^2(\frac{1}{2}\theta)]^2}F_1^nF_2^n+\tfrac{1}{16}q^2\frac{\sin^2\theta}{[1+\frac{1}{2}q^2\sin^2(\frac{1}{2}\theta)]^2}(F_2^n)^2\Bigg], \tag{4.23a}$$

where

$$F_s^n=\sum_{l=-\infty}^{+\infty}J_l\left(\tfrac{1}{4}nq^2\frac{\sin^2(\frac{1}{2}\theta)}{1+\frac{1}{2}q^2\sin^2(\frac{1}{2}\theta)}\right)\times\left[J_{2l+n+s}\left(\frac{qn\cos\alpha}{1+\frac{1}{2}q^2\sin^2(\frac{1}{2}\theta)}\right)+J_{2l+n-s}\left(\frac{qn\cos\alpha}{1+\frac{1}{2}q^2\sin^2(\frac{1}{2}\theta)}\right)\right]. \tag{4.23b}$$

We can expand (4.23) to low order in q^2 and find the leading term for $n\geq 2$. [For $n=1$ the leading term is simply the linear polarization version of Thomson scattering, i.e., (3.16) with $\delta^2=1, 0$.] The leading term then becomes

$$dP_L^{(n)}/d\Omega_L=n^2A(\omega_L^2)\times[\sin^2\alpha(F_1^n)^2-\tfrac{1}{2}q\cos\alpha\cos\theta\, F_1^nF_2^n+\tfrac{1}{16}q^2\sin^2\theta(F_2^n)^2], \tag{4.24a}$$

where

$$F_r^n=(\tfrac{1}{2}q)^{n-r}\sum_{l=0}^{L_r}\frac{(-1)^l}{l!}[\tfrac{1}{2}n\sin^2(\tfrac{1}{2}\theta)]^l\frac{(n\cos\alpha)^{n-r-2l}}{(n-r-2l)!} \tag{4.24b}$$

and L_r is that value of l that makes $n-r-2l$ either 0 or 1.

For low q^2 we can expand beyond the leading term. To order q^4, we find for the first three harmonics

$$dP_L^{(1)}/d\Omega_L=A(\omega_L^2)[1+\tfrac{1}{2}q^2\sin^2(\tfrac{1}{2}\theta)]^{-4}\times\{\sin^2\alpha+q^2(A_1-\tfrac{1}{2}\cos_2\alpha\cos\theta)+q^4[A_2-A_1-\tfrac{3}{4}\sin^4(\tfrac{1}{2}\theta)\cos^2\alpha+\tfrac{1}{2}\sin^2(\tfrac{1}{2}\theta)\cos^2\alpha-\tfrac{1}{16}\cos^2\alpha\sin^2\theta-\tfrac{1}{8}\cos^2\alpha\sin^2(\tfrac{1}{2}\theta)\cos\theta+\tfrac{1}{4}\cos^4\alpha\cos\theta-\tfrac{1}{32}\sin^2\alpha\sin^2\theta]\}, \tag{4.25a}$$

where

$$A_1=\tfrac{1}{4}[-\sin^2\alpha\cos^2\alpha-\sin^2\alpha\sin^2(\tfrac{1}{2}\theta)+\cos^2\alpha\cos\theta],$$

$$A_2=\tfrac{5}{32}\sin^2\alpha\cos^2\alpha\sin^2(\tfrac{1}{2}\theta)-\tfrac{1}{64}\sin^2\alpha\sin^2(\tfrac{1}{2}\theta)+(5/192)\cos^4\alpha\sin^2\alpha-\tfrac{1}{8}\cos^4\alpha\cos\theta-\tfrac{1}{32}\cos^2\alpha\sin^2(\tfrac{1}{2}\theta)\cos\theta+\tfrac{1}{64}\sin^2(\tfrac{1}{2}\theta)\cos^2\alpha;$$

$$dP_L^{(2)}/d\Omega_L=4q^2A(\omega_L^2)\times[C_1+q^2(C_2-3\sin^2(\tfrac{1}{2}\theta)C_1-\tfrac{1}{4}\cos^4\alpha\cos\theta+\tfrac{1}{8}\cos^2\alpha\sin^2\theta]), \tag{4.25b}$$

where

$$C_1=\sin^2\alpha\cos^2\alpha-\tfrac{1}{2}\cos^2\alpha+\tfrac{1}{16}\sin^2\theta,$$

$$C_2=\tfrac{2}{3}\cos^4\alpha\cos\theta-\tfrac{2}{3}\sin^2\alpha\cos^4\alpha-\tfrac{1}{8}\sin^2\theta\cos^2\alpha;$$

$$dP_L^{(3)}/d\Omega_L=(81/64)A(\omega_L^2)q^4\times[\tfrac{1}{4}\sin^2\alpha(1-\cos\theta-6\cos^2\alpha)^2+\sin^2\theta\cos^2\alpha+\cos^2\theta\cos^2\alpha(1-\cos\theta-6\cos^2\alpha)]. \tag{4.25c}$$

The corresponding total powers radiated at these harmonics are

$$P_L^{(1)}=A(\omega_L^2)\left[\left(\frac{8\pi}{3}-\frac{9\pi}{5}q^2+\frac{1311\pi}{1120}q^4\right)+\left(-\frac{4\pi}{3}q^2+\frac{227\pi}{120}q^4\right)\right], \tag{4.26a}$$

$$P_L^{(2)}=A(\omega_L^2)\left[\left(\frac{14\pi}{5}q^2-\frac{138\pi}{35}q^4\right)-\left(\frac{\pi}{15}q^4\right)\right], \tag{4.26b}$$

$$P_L^{(3)}=A(\omega_L^2)[(621\pi/224)q^4], \tag{4.26c}$$

where these quantities are written in such a way that the first parenthesis gives the result in the R frame[17] and the second gives the corrections for transforming into the L frame and for the difference between emitted and observed power.

As we go to higher and higher q^2, the angular distribution changes from predominantly backward to more and more forward. This may be understood by looking at Fig. 1. At low q^2, the R- and L-frame results are the same since the drift velocity is of order q^2. The electron radiates most on the curved portion of the figure eight, and on this portion, the electron is going backward. The radiation of the higher harmonics is

[17] E. S. Sarachik and G. T. Schappert, Nuovo Cimento Letters **2**, 7 (1969).

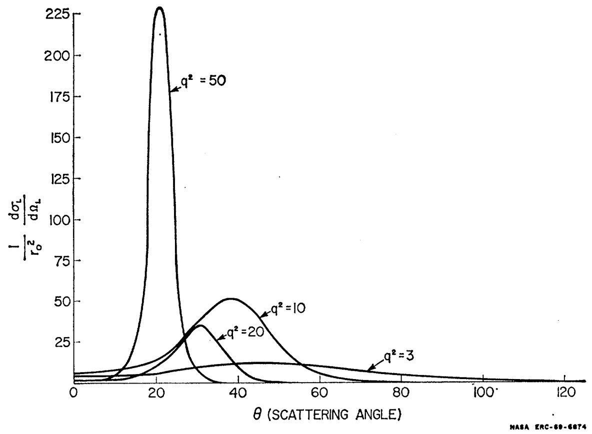

FIG. 3. Plot of the total observed power cross section in the laboratory for various incident intensities. The scale for the $q^2=3$ and 10 curves is one-fifth that shown here.

therefore backward peaked at low q^2. As q^2 increases, the drift velocity always increases faster than any internal velocity characteristic of the figure eight so that the radiation becomes more and more forward peaked. We expect the same qualitative behavior of the high-q^2 radiation as in the circularly polarized case.

V. CONCLUSIONS

We have investigated the motion and subsequent radiation of an electron (or any charged particle) subject to an intense optical field. We have obtained an exact solution (3.12) and (3.15) for the expected observed power for arbitrary intensity and elliptic polarization of the incident optical field. Our two major assumptions have been that the problem could indeed be treated classically and that we could decouple the problem into a motion part and a radiation part within the classical approximation by neglecting radiation reaction. We will discuss these and other assumptions briefly in this section.

That classical theory works for this problem has been shown by Brown and Kibble[3] and been reviewed by Kibble.[4] The incident frequency must be such that $\hbar\omega \ll mc^2$, a condition that is clearly satisfied for incident optical radiation. The meaning of the condition is that the incident photons must not individually have enough energy to cause the electron to recoil. So too in the emission of an nth harmonic photon, classical theory cannot account for the recoil of the electron so that we must impose the restriction $n\hbar\omega \ll mc^2$ in order for our treatment to be valid. We see that for incident radiation of $\hbar\omega \sim 1$ eV, our theory no longer holds for harmonics higher than about 10^5. Note that this restriction is independent of the intensity. We have already seen that the neglect of radiation reaction requires that $q^2 \ll \lambda/r_0$ which means that $q^2 \ll 10^9$ at optical frequencies. This clearly is a very loose restriction and need not concern us further.

We have made some assumptions about the pulse length of the incident radiation that can be made more explicit. The pulse length must be taken long enough for there to be many optical cycles contained within it. Thus the pulse must be longer than about 10^{-13} sec. For pulses shorter than this, the averaging we performed can no longer be done. In addition to this averaging problem, we must realize that a pulse in the vector potential is no longer the same pulse in the electric field at these short times and we must begin to ask ourselves which one really comes out of a pulsed laser.

The pulse also cannot be too long—the longitudinal drift distance $\frac{1}{4}q^2Tc$ of the electron must be small compared to the scale of the experimental apparatus so that the angle of the scattered radiation be well defined. Since at $q^2=1$ a picosecond pulse corresponds to a drift distance of only 0.03 cm, this leaves us considerable leeway. However, an increase of intensity by several orders of magnitude would require still shorter pulses.

Finally, let us remember that our calculations have dealt with scattering from a single electron. In an actual experiment, an electron beam or a plasma would be used to provide the electrons. When many electrons are present, we might expect the usual coherence effects in the forward direction. Since we have seen that only the fundamental frequency is scattered forward, we conclude that there are no coherence effects for the higher harmonics. Other plasma effects would be expected to enter only if the density of the electron beam approached that of a metal. In most experimental situations, the density would be such that the plasma frequency is far less than an optical frequency, so that plasma effects would not enter to change the conclusions of this paper.

ACKNOWLEDGMENTS

We would like to thank Dr. Kenneth Billman for interesting us in this problem and for his constant encouragement and support. We would also like to thank Dr. David Burnham for many helpful discussions. One of us (GTS) wishes to thank Professor T. W. B. Kibble for valuable discussions.

APPENDIX

In the body of the paper, we have expressed our results in terms of the power angular distribution $dP^{(n)}/d\Omega$. This quantity seemed the most natural one to use since it corresponds most closely to what an experiment would actually measure. Since other quantities, namely, power cross sections and number cross sections, have appeared in the literature, we will here clarify the relations between all these quantities.

In a given frame, the power cross section is defined as $(1/I)\,dP/d\Omega$ where I, the incident intensity, is given as $e^2q^2\omega^2/8\pi cr_0^2$. We have written the equations in the text of the paper in such a way that replacing $A(\omega^2)$ by r_0^2 and $B(\omega^2)$ by $(8/3)\pi r_0^2$ changes the expressions for

$dP^{(n)}/d\Omega$ and $P^{(n)}$ into those for $d\sigma^{(n)}/d\Omega$ and $\sigma^{(n)}$ (the corresponding power cross sections), respectively.

The third quantity, the number cross section, appears the least useful from the experimental point of view yet has appeared in some of the standard papers on the subject, since it is most natural from the point of view of quantum-mechanical calculations. The differential number cross section in a given frame, $d\Sigma^{(n)}/d\Omega$, is defined as the number of nth harmonic photons detected in a solid angle $d\Omega$ divided by the number of (first-harmonic) incident photons all in some unit time interval. In a given frame, the relation is easily seen to be

$$\begin{aligned} d\Sigma^{(n)}/d\Omega &= (\omega^0/\omega_{\text{scat}})(d\sigma^{(n)}/d\Omega) \\ &= (\omega^0/\omega_{\text{scat}})(1/I)(dP^{(n)}/d\Omega). \end{aligned} \quad \text{(A1)}$$

In particular, in the L frame this relation becomes

$$\frac{d\Sigma_L^{(n)}}{d\Omega_L} = \frac{1}{n}[1+\tfrac{1}{2}q^2\sin^2(\tfrac{1}{2}\theta)]\frac{1}{I_L}\frac{dP_L^{(n)}}{d\Omega_L}. \quad \text{(A2)}$$

If we compare our results to those of Brown and Kibble,[3] we note that it is the number cross section derived from the power lost by the electron that agrees precisely with their results. They did not consider the extra time retardation that must be included when going from the power lost by the electron to the power observed in a given frame. It is the observed power rather than the power lost by the electron that is actually measured so that this extra retardation must be included when comparing theory to experiment.

PHYSICAL REVIEW D VOLUME 1, NUMBER 10 15 MAY 1970

New Dynamical Group for the Relativistic Quantum Mechanics of Elementary Particles*

J. J. Aghassi, P. Roman, and R. M. Santilli
Department of Physics, Boston University, Boston, Massachusetts 02215
(Received 13 November 1969)

Nonrelativistic Galilean quantum mechanics and the standard transition to relativistic Poincaré quantum mechanics is analyzed in terms of group theory. Special emphasis is given to the discussion of the relation between dynamics and geometry. Certain unsatisfactory features are pointed out and a new relativistic group $\mathcal{G}_5$ is suggested as the symmetry group of dynamics. $\mathcal{G}_5$ contains both the nonrelativistic Galilei group and the Poincaré group as subgroups, and it is a group extension of the restricted Lorentz group. For use in relativistic quantum mechanics, the central extension of $\mathcal{G}_5$ by a phase group must be employed. The Lie algebra of this relativistic quantum-mechanical Galilei group $\tilde{\mathcal{G}}_5$ contains an acceptable covariant space-time position operator and a nontrivial relativistic mass operator. The latter also serves to describe dynamical development. The irreducible unitary projective representations of $\tilde{\mathcal{G}}_5$ correspond to infinite towers of states with increasing spin.

I. GROUP-THEORETICAL ANALYSIS OF NONRELATIVISTIC QUANTUM MECHANICS

Undoubtedly, the most remarkable feature of relativistic dynamics is that the invariance group of the dynamical law coincides with the group of rigid motions (essentially the group of isometries) of the underlying geometrical manifold. In fact, the underlying geometrical manifold is the Minkowski space $E_{3,1}$ where the identity component of the group of isometries is the connected Poincaré group containing the identity, i.e., the inhomogeneous Lorentz group[1] $ISO_0(3,1)\equiv T_4\otimes\mathcal{L}_+^\uparrow$. At the same time, the laws of motion are required to be invariant under $ISO_0(3,1)$. The situation is very different in nonrelativistic physics. The underlying geometrical manifold is, to start with, the Euclidean space E_3, where the identity component of the group of isometries is the connected Euclidean group, i.e., the inhomogeneous rotation group $ISO(3)\equiv T_3\otimes SO(3)$. This space does not permit even the formulation of any dynamics. One therefore introduces the time as an additional kinematical variable and thereby changes the underlying manifold from E_3 to $E_3\times E_1$. Note that no metric is introduced into this Cartesian product space. Next one demands that the laws of motion be invariant under the connected component of the Galilei group. This group we shall denote in what follows by the symbol $\mathcal{G}_4$. The carrier space of $\mathcal{G}_4$ is $E_3\times E_1$ and the group is obtained by adjoining to the transformations of $ISO(3)$ the additional two sets of transformations

$$x_k\to x_k+v_kt, \quad \text{(1.1a)}$$

$$t\to t+\tau, \quad \text{(1.1b)}$$

* Work supported by the U.S. Air Force under Grant No. AFOSR-67-0385B.

[1] For convenience, in this paper we shall use the symbol $SO_0(3,1)$ for the restricted Lorentz group $\mathcal{L}_+^\uparrow$, even though this notation is not quite standard.